PROCEEDINGS

OF THE

FIFTH SYMPOSIUM

ON THE

GEOLOGY OF THE BAHAMAS

Edited by

Roger J. Bain

Production Editor

Donald T. Gerace

Bahamian Field Station
San Salvador, Bahamas
1991

Printed in USA by Don Heuer

ISBN 0-935909-37-0

Measurements of Tidal Water Table Fluctuations in Well Field North of Cockburn Town, San Salvador, Bahamas

Gerhard Kunze, Thomas J. Quick, and Gayla D. Gross
Department of Geology
University of Akron
Akron, OH 44325-4191

ABSTRACT

Water level fluctuations were measured in seven wells near the Cockburn Town airstrip in July 1989, December 1989 and January 1990, using a custom built tide gauge. Results indicate prominent tidal cycles in four of the wells with tidal ranges of approximately 1/2 m. Water level fluctuations in the other three wells are irregular and appear to be unrelated to the tides. Comparison of observed well tides with predicted ocean tides indicates tidal lag times ranging from 20 to 30 minutes and tide attenuation ranging from about 20% to over 50%. Lag times and tidal attenuations show no correlation with distance from the coast and are not compatible with the tidal attenuation model by Ferris (1951), according to which tidal range ratios (R/Ro) and lag times (t_L) are related as

$$R/Ro=\exp(-2\pi t_L/t_0)$$

where t_o is the tidal period. Aquifer transmissivities corresponding to observed tidal lag times and range ratios are unrealistically high and range from 30 to over 100 m^2/s. Maximum transmissivities implied by the absence of tidal fluctuations in the three other wells are on the order of 1 m^2/s. These unexpected results may be attributable to a peculiar system of subsurface caves or conduits, pumping of wells during measurement periods, incorrect tide tables, effects of atmospheric pressure fluctuations, unmodeled precipitation events, equipment malfunction, or a combination of these factors. Another possibility is that the Ferris model is not applicable to Bahamian karst hydrology.

The tide gauge used is a custom built unit utilizing changes in air pressure in a submerged sensing element due to changes of the height of the water column. Major sources of error in this device appear to be air leaks in tube connectors and calibration problems. A new type of tide gauge developed in order to eliminate these sources of error uses changes in sensor capacitance due to water level changes.

INTRODUCTION

Coastal and small-island aquifers undergo tidal fluctuations that depend on various factors such as distance from the ocean, coast geometry, aquifer transmissivity and the nature of the aquifer (confined, semiconfined, or unconfined), among others. The idealized case of tidal fluctuations in a thin, confined aquifer in contact with ocean tides along a straight coast was treated by Ferris (1951) who determined the resulting fluctuations of the piezometric groundwater surface to be of the form

Equation (1)

$$h(x,t)=h_0\exp(-x\sqrt{\pi S/t_0T})\sin(2\pi t/t_0-x\sqrt{\pi s/t_0T})$$

where h(x,t) is the aquifer tidal piezometric level at time t and distance x from the coast, h_o is the amplitude (half range) of the coastal tidal component of period t_o, and S and T are the storage coefficient and transmissivity of the aquifer, respectively. Accordingly, the tidal range decreases inland exponentially as

Equation (2)

$$h(x)/h_0=R(x)/R_0=\exp(-x\sqrt{\pi s/t_0T})$$

where the R are the tidal ranges inland and at the coast, and the corresponding tidal fluctuations undergo a time lag given by

Equation (3)

$$t_L=x(t_0S/4\pi T)^{\frac{1}{2}}$$

equations (1) and (2) may be expressed in terms of the tidal lag time t_L as

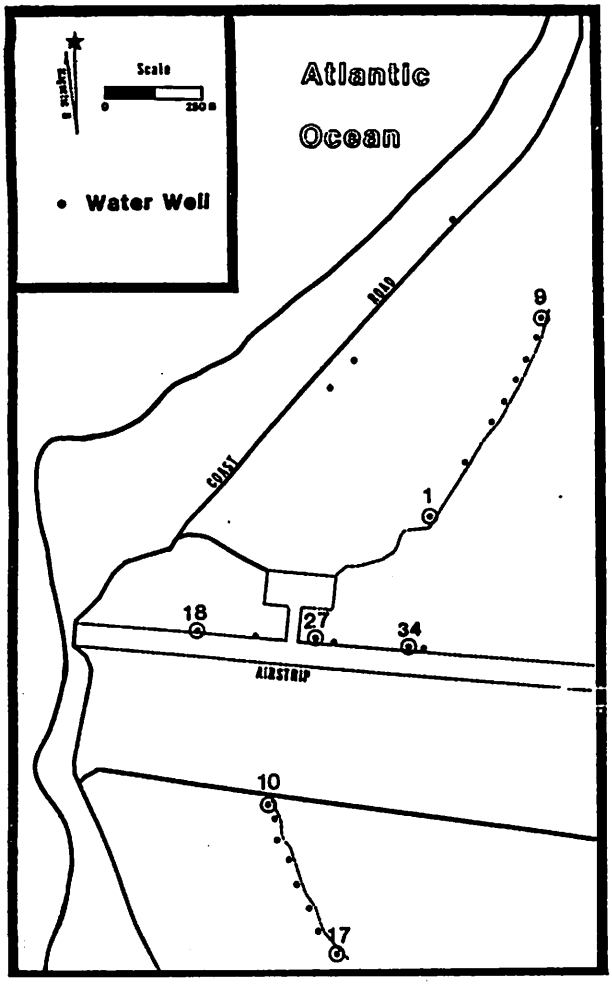

Fig.1 Well field near Cockburn Town airstrip. Wells numbered 1 through 9 and 10 through 17 are uncased test wells, wells 18-35 are cased production wells along the runway.

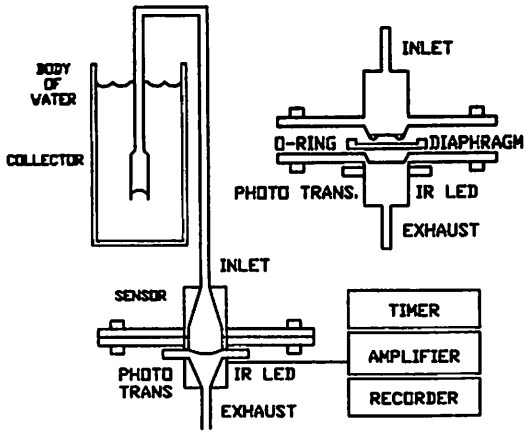

Fig.2 Air pressure tide gauge.

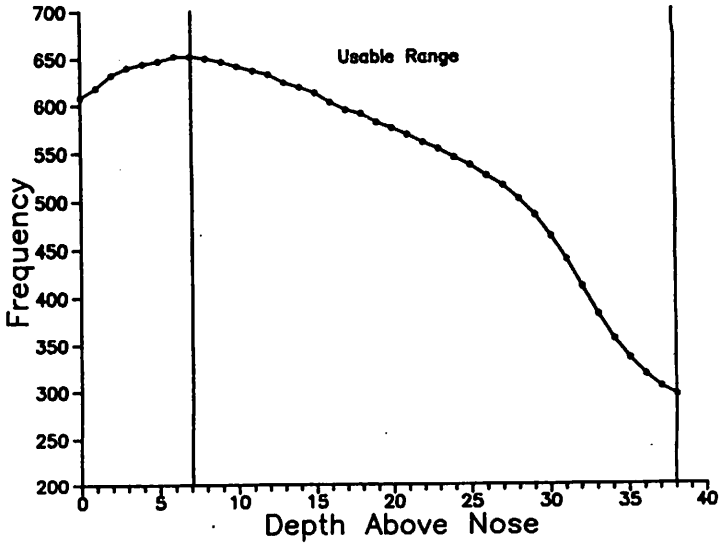

Fig.3 Tide gauge calibration curve.

Equation (4)

$$h(x,t)=h_0\exp(-2\pi t_L/t_0)\ \sin 2\pi(t-t_L)/t_0$$

and

Equation (5)

$$R(x)/R_0=\exp(-2\pi t_L/t_0)$$

Although these equations represent the behavior of confined aquifers, they are also applicable to unconfined aquifers if the range of tidal fluctuations is small compared to the saturated thickness of the aquifer (Todd, 1959; Vacher, 1978). This condition is met by the phreatic zone of San Salvador Island.

INSTRUMENTATION AND PROCEDURES

Study Area

This investigation deals with the analysis of tidal water level oscillations in the well field around the Cockburn Town airstrip, San Salvador, Bahamas (Fig. 1). Wells 1 through 9 (northern line) and 10 through 17 (southern line) are uncased 10 cm (4 in.) diameter test wells extending to a maximum depth of approximately 6 m below the water table. Wells 18 through 34 (along the runway) are 20 cm (8 in.) diameter, partially cased production wells extending 3-4 m below the water table. The northern line runs along the eastern flank of a low eolianite ridge

Table 1. General well data

Well Number	Elevation (m)	Total Well Depth (m)	Salinity (ppm)	Date
1	3.5	8.8	475	12/28/89
9	2.3	7.0	1760	07/04/89
10	3.8	9.0	1000	12/31/89
17	3.8	9.0	1000	07/05/89
18	1.2	5.0	700	07/03/89
27	1.4	5.0	unk.	01/02/90
34	2.0	5.0	325	12/30/89

Table 2. San Salvador Ocean Tides

Date	Time (EST)	Height of Tide (cm)	Well Number
03 Jul 89	13:37	0 *	18
	20:09	87 *	
04 Jul 89	02:27	0 *	
	08:37	70 *	
	14:28	3 *	9
	20:55	84 *	
05 Jul 89	03:11	0 *	
	09:23	70 *	17
	15:15	3	
	21:37	79	
06 Jul 89	03:43	0	
28 Dec 89	14:09	-8	1
	20:12	50	
29 Dec 89	01:55	-8 *	
	08:29	70 *	
	14:46	-8 *	
	20:50	53 *	
30 Dec 89	15:20	-8	34
	21:31	56	
31 Dec 89	03:22	-6	
	09:49	70	
	16:01	-6	
	22:14	62 *	10
01 Jan 90	04:03	-3 *	
	10:22	73 *	
	16:38	-6 *	
	22:54	67	
02 Jan 90	04:56	0	
	11:10	67	27
	17:23	-6	
	23:46	67	
03 Jan 90	05:55	0	

Notes: 1. Tide data from NOAA tide tables
2. Asterisks denote values used in calculation of tidal coefficients

Table 3. Amplitude and phase relationships of coastal tides

Date-time-group	Reference Tide	Reference Well	A (cm)	B (cm)	C (cm)	ϕ_2 (rad)
07-03-13:37	LW	18	39.2	-39.2	8.5	1.57
07-04-14:28	HLW	9	39.2	-37.8	7.2	1.36
12-29-01:55	LW	1	26.8	-34.8	8.5	1.57
12-31-22:14	LHW	10	31.5	36.0	5.7	2.88

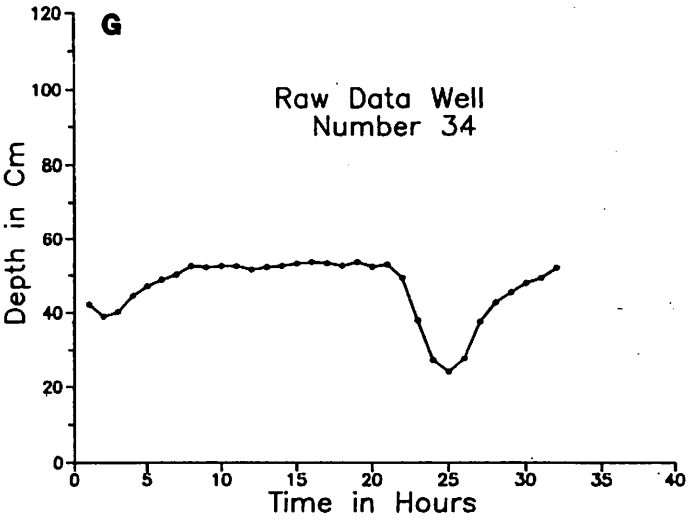

Fig.4 Water level fluctuation in well 34(G).

of approximately 8 m maximum elevation, and the southern line crosses low ridges and swales of 5 m maximum elevation. The production wells along the runway are within 2 m of mean sealevel. Well elevation data are given in Table 1.

Equipment

The tide gauge used (Fig. 2) operates as follows: a submerged inverted cylindrical collector unit is connected to a pressure transducer by 1/8 inch flexible plastic tubing. Water level changes cause pressure changes in the tube that are transmitted to a thin rubber diaphragm which bulges as a function of pressure and partially obstructs the path of an infrared beam of an optical sensor inside the pressure transducer. Changes in the intensity of the IR beam reaching the detector cause an A/D (analog-to-digital) converter to change the frequency of an electric current which is recorded on standard cassette tape. The device is controlled by a quartz clock set to record a 5-second sample each hour. Decoding is accomplished by playback through a frequency counter. The instrument is calibrated by direct measurement of the changing frequency as the collector unit is lowered through a column of water in the laboratory. The calibration curve used in this investigation is shown in Figure 3. Possible sources of error in this device are air leaks in tube connectors, the effects of air pressure and temperature changes, and calibration problems.

Water levels were recorded in wells 1, 9, 10, 17, 18, 27 and 34 (see Figure 1) over periods ranging from 19 to 40 hours starting on the dates

Table 4. Well tide parameters

Parameter	Well 1	Well 2	Well 10	Well 18
Record start	28-16:20	04-12:50	31-19:20	03-15:50
Reference tide	LLW	LLW	LHW	LLW
Reference time	29-02:15	04-15:00	31-22:40	03-14:20
H1 (cm)	46	43	107	0 *
H2 (cm)	93	91 *	55	67
H3 (cm)	54	64	111	8
H4 (cm)	80	86	51	44
b (cm)	-18.3	-17.5	28.1	-28.0
c (cm)	7.6	10.8	2.8	12.2
Diurnal phase	2.12	2.91	2.36	1.91
$\Delta\phi_2$ (rad)	0.5	1.55	-0.55	0.34
t_1 (h)	0.5	0.4	0.4	0.5
t_2 (h)	2.7	7.5	-1.8	2.8

Notes: 1. Asterisks denote estimated values

2. Semidiurnal lag times t_1 are averages over one tidal period

Table 5. Attenuated well tide range ratios

Well	Distance from Coast	Semidiurnal Ratio		Diurnal Ratio	
1	620 m	0.53	(0.78)	0.89	(0.64)
9	450 m	0.46	(0.82)	1.50	(0.58)
10	520 m	0.78	(0.82)	0.49	(0.84)
18	330 m	0.71	(0.78)	1.47	(0.78)

Table 6. Hydrological parameters implied by well tides

Well	Distance from Coast (m)	Semidiurnal Lag Time (h)	Hydraulic Transmissivity (m^2/s)	Hydraulic Conductivity (m/s)
1	620	0.5	105	3.0
9	450	0.4	87	2.5
10	520	0.4	116	3.3
17	700	8.0	0.53	0.016
18	330	0.5	30	0.9
27	650	8.0	0.45	0.013
34	920	8.0	0.91	0.026

given in Table 1. The resulting water level fluctuations are shown in Figure 4. Prominent tidal cycles are evident in wells 1, 10, 18, and possibly 9 (Fig. 4A, 4C, 4E and 4B). Irregular water level fluctuations were recorded in the other wells. There is no obvious correlation between tidal activity and well water salinities.

ANALYSIS

Table 2 shows ocean tides promulgated for San Salvador in the Tide Tables published by the U. 5. Department of Commerce during the time periods of these well measurements. In general, the time series representing these mixed tides during one tidal day of 24.833 hours can be expressed as

Equation (6)

$$H(t)=A+B\cos(w_1t-\phi_1)+C\cos(w_2t-\phi_2)$$

where A is the average departure of sealevel from MSL (mean sealevel) during the tidal period, B is the amplitude of the semidiurnal component of angular frequency w_1 (0.5060/h using a semidiurnal period of 12.4167h), and C is the amplitude of the diurnal component of angular frequency w_2 (0.2530/h). Φ_1 and Φ_2 are phase factors. If the tidal period is chosen to begin with either a tidal peak or trough, then Φ_1 equals zero. In that case the tidal time series can be written as

Equation (7)

$$H(t)=A+B\cos w_1t+C'\sin w_2t+D'\cos w_2t$$

and the four coefficients A, B, C', D' are calculated from the published tidal extremum values H_1, H_2, H_3, and H_4 as follows:

Equation (8a)

$$A=(H_1+H_2+H_3+H_4)/4$$

Equation (8b)

$$B=(H_1+H_3)/2-A$$

Equation (8c)

$$C'=(H_2-H_4)/2$$

Equation (8d)

$$D'=(H_1-H_3)/2$$

From these coefficients the amplitude and phase of the diurnal component (in equation 6) are determined as

Equation (9a)

$$C=(C'^2+D'^2)^{1/2}$$

Equation (9b)

$$\phi_2=Arctan(C'/D')$$

Application of these equations to the coastal tide data of Table 2 results in the tidal amplitudes and phases listed in Table 3. In view of the fact that only wells 1, 9, 10 and 18 show clear tidal oscillations, Table 3 lists only the ocean tides corresponding to the dates of these four well observations. The reference tides represent extrema immediately preceding corresponding well tide extrema.

According to equations (1) and (3), well tides are delayed by a lag time t_L that is a function of the tidal period t_o. Thus diurnal and semidiurnal components are delayed by differing lag times t_1 and t_2 which cause different additional phase shifts ϕ'_1 and ϕ'_2. Where $\phi'_1 = w_1 t_1$ and $\phi'_2 = w_2 t_2$. The corresponding well tide time series may be written as

Equation (10)

$$H(t)=a+b\cos(w_1t-\phi'_1)+c\cos(w_2t-\phi_2-\phi'_2)$$

or, if referred to the delayed reference extremum corresponding to that used to calculate the time series for the ocean tide,

Equation (11)

$$H(t)=a+b\cos w_1t+c\cos(w_2t-\phi_2-\Delta\phi_2)$$

where $\Delta\phi_2 = w_2(t_2-t_1)$. Using calculations analogous to those of equations (8) and (9), the tidal coefficients, phases and lag times of wells 1, 9, 10, and 18 are determined as listed in Table 4. The semidiurnal lag time t_1 is determined directly by comparing the times of corresponding extrema of ocean and well tides. The value of t_2 is calculated from the phase of the diurnal well component.

DISCUSSION

The determination of lag time t_1 depends critically on the proper identification of corresponding phases in ocean and well tides. Due to the expected differential phase delay between semidiurnal and diurnal components as the tide propagates inland, the shape of the tidal curve changes, and proper identification becomes ambiguous. Thus in wells 1 and 18 this differential phase shift probably explains the change of a coastal LW (low water) phase to a LLW (lower low water) phase, but the change of a HLW (higher low water) phase to a pronounced LLW phase in well 9 is less believable. However, the HLW phase in well 9 occurs approximately 13 hours after the coastal HLW phase. According to equation 5 the attenuated amplitude ratio corresponding to such a large semidiurnal phase lag is less than 0.002. Hence, the only phase in well 9 that could possibly correspond to the coastal HLW tide is the LLW tide. In general, perceptible tides with tidal ranges of at least several cm (or range ratios greater than 2%) must have semidiurnal lag times (t_1) of less than approximately 8 hours. A similar restriction (15 hours) holds for the diurnal component, and the large diurnal component in well 9 is incompatible with the large lag time of 7.5 hours (which corresponds to an attenuated amplitude ratio of 0.15). Similarly the negative lag time (or lead time) calculated for well 10 may actually represent an impossibly large positive lag time of approximately 23 hours, either of which has no reasonable explanation in terms of our hydrologic model. In fact, none of the diurnal lag times t_2 conform to the Ferris model which predicts that, according to equation 3, diurnal and semidiurnal lag times should be related as

Equation (12)

$$t_2 = t_1(2)^{1/2}$$

Comparison of semidiurnal and diurnal coefficients of well and ocean tides permits determination of tidal amplitude attenuation in the form of reduced amplitude ratios b/B and c/C. The results, shown in Table 5, are quite

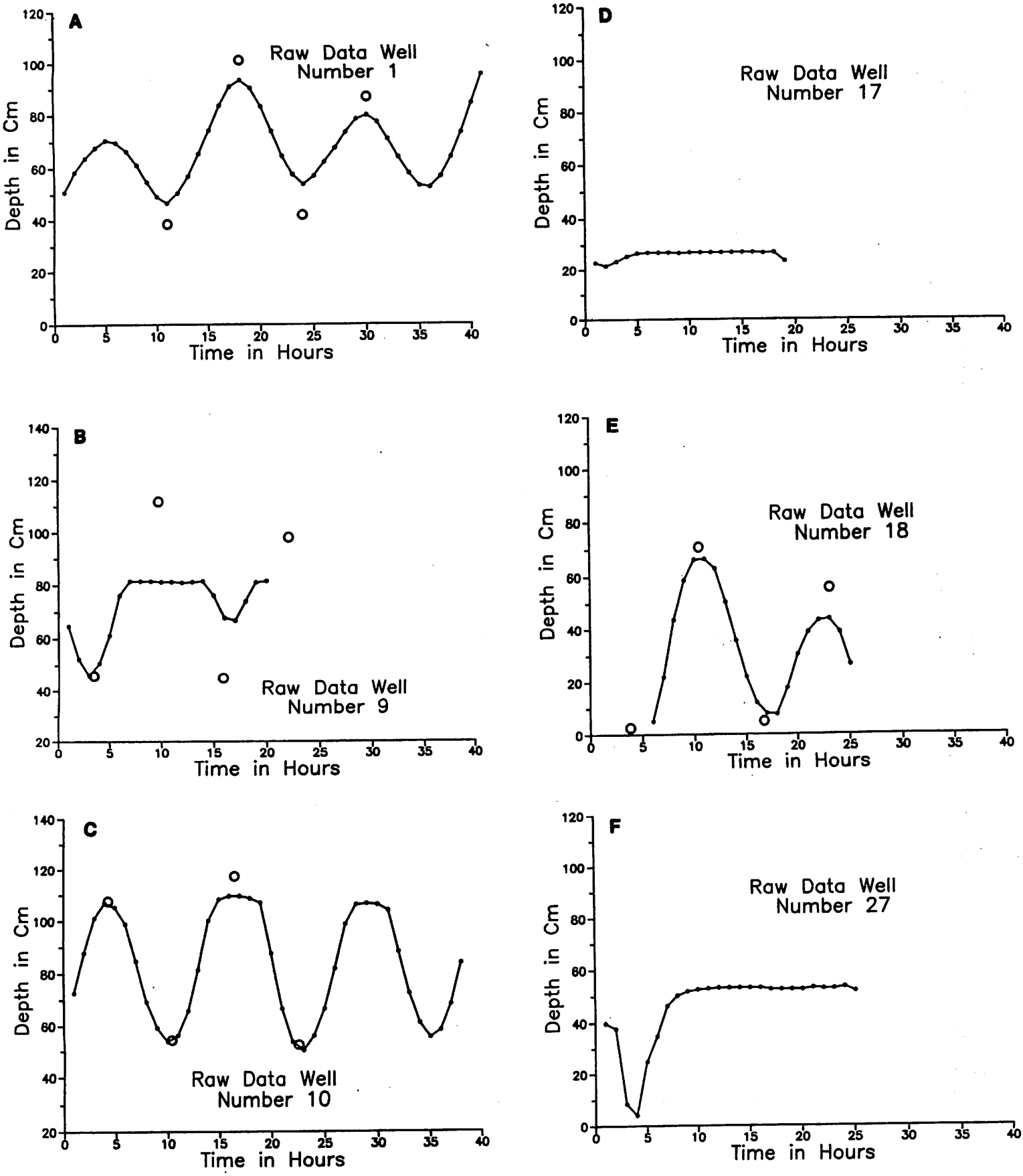

Fig.4 Water level fluctuation in wells 1(A), 9(B), 10(C), 17(D), 18(E), 27(F). Theoretical values are shown by circles.

unexpected. Well 10, the second most distant well from the coast, shows the smallest amplitude attenuation with a reduced semidiurnal amplitude ratio of 0.78 (or an attenuation of 22%). The amplitude ratios given in parentheses are theoretical values, corresponding to the observed semidiurnal lag times, calculated using equation 5. Clearly the observed values do not agree with the Ferris model. Even more puzzling are the diurnal data. According to the Ferris (1951) model, the attenuation of the diurnal tidal component should be less than that of the semidiurnal component. In fact, in view of equation 2, the diurnal and semidiurnal range ratios at a given well should be related as

Equation (13)

$$c/C = (b/B)^{.707}$$

The resulting theoretical values are also listed in parentheses (in the last column of Table 5). Again, the observed diurnal attenuations as well as the diurnal lag times are incompatible with the Ferris model. Thus the diurnal range ratio for well 10 is smaller than that of the semidiurnal component. In contrast, the diurnal range ratios for wells 9 and 10 are greater than one, implying an actual enhancement of the diurnal component in those wells. Although such tidal enhancements have been reported in the literature (e.g. Cant, 1989; Davis and Johnson, 1989) and might be explained by peculiar aquifer or cave plumbing, it appears more likely that the recorded well data are in error. The shapes of the recorded well level curves (Fig. 4) support this suspicion. Only wells 1 and 18 display convincing sinusoidal fluctuations, whereas the peaks of the other curves appear uncharacteristically flattened. Again, this could be due to peculiar aquifer characteristics, but malfunction of the experimental equipment or faulty instrument calibration are more likely causes.

Notwithstanding probable errors in determining well tide amplitudes, the recorded times of semidiurnal tidal extrema in the wells are more reliable, and this allows reasonably accurate determination of corresponding tidal lag times (t_1) and related hydrological parameters. The calculated diurnal tidal lag times (t_2) are not realistic because the pertinent calculations are highly sensitive to errors in recorded tide levels, or because the data are affected by non-tidal diurnal effects such as water table fluctuations in response to evapotranspiration. This effect may be particularly important in wells 9 and 18 where the water table is close to the surface.

The Ferris model predicts that tidal lag times and attenuations are related according to equation 5. Figure 5 is a parametric plot of this functional relationship for the semidiurnal component. The observed values for wells 1, 9, 10, and 18 are shown as stars. All observed amplitudes are below the theoretical curve, signifying either erroneous measurements or an incorrect hydrological model. It might be worth noting that if the recorded water level curves in wells 9 and 10 had fully developed (sinusoidal) peaks, the resulting semidiurnal amplitudes would conform better to the theoretical trend, especially for well 9. The theoretical attenuated well tides based on the observed semidiurnal lag times t_1 and corresponding diurnal lag times t_2 (calculated in accordance with equation 12) are shown by circles representing extremum values on Figure 4.

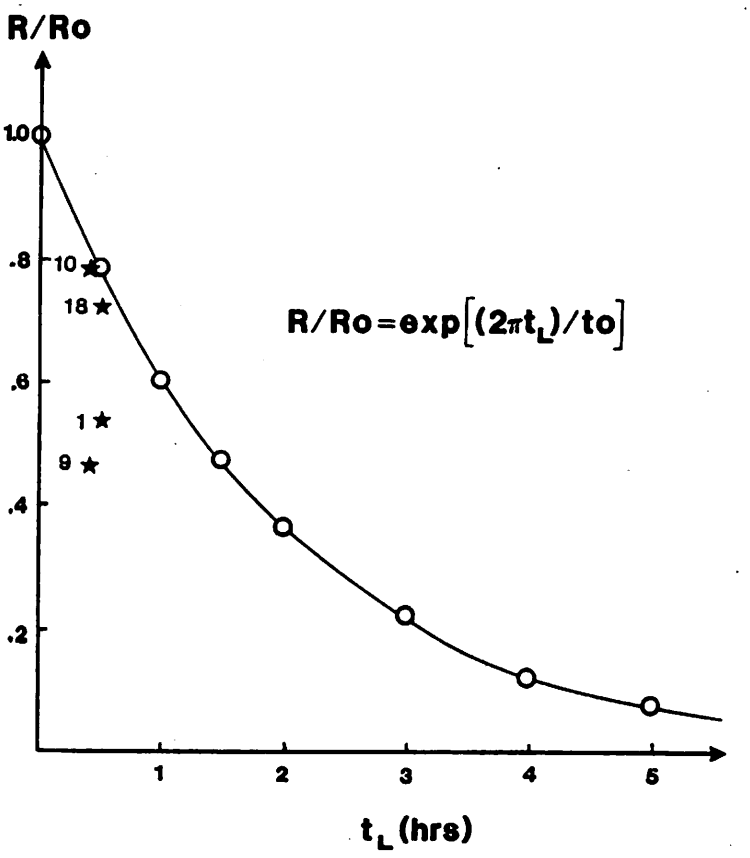

Fig.5 Theoretical and observed (stars) amplitude vs. lag time relationships for the semidiurnal tidal component.

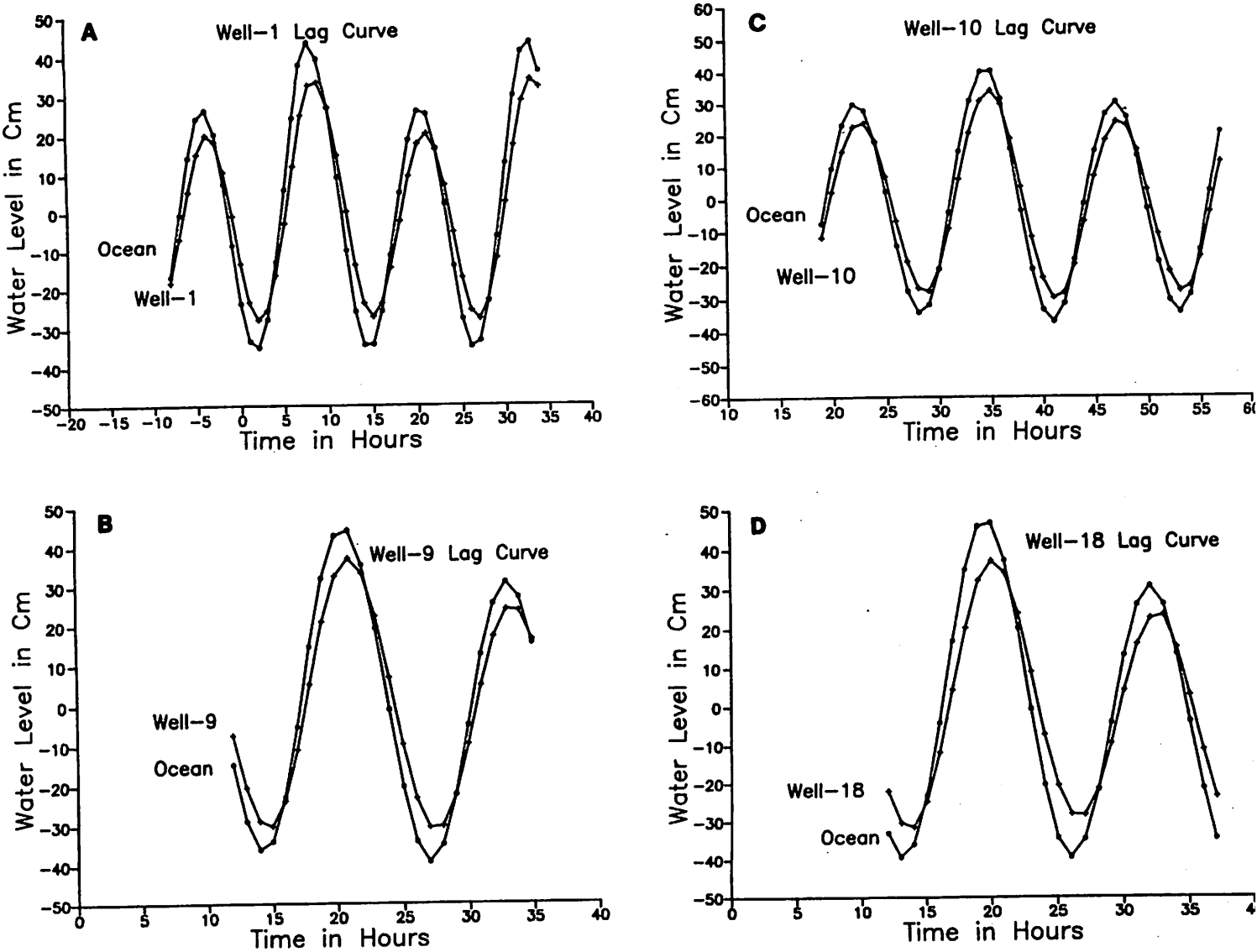

Fig.6 Relationship between ocean tides and theoretical attenuated well tides in wells 1(A), 9(B), 10(C), and 18(D).

Theoretical and observed amplitudes show close agreement in well 10; with less agreement in the other wells. Figure 6 shows the ocean tides superimposed on the theoretical attenuated well tides.

Wells 17, 27 and 34 show irregular, in some cases (wells 27 and 34) significant water level fluctuations that appear to be unrelated to the tides. Prominent lows in the water level record of these wells occur from 7 to 11 hours after preceding coastal low tides. According to equation 5, lag times of this magnitude correspond to tidal attenuations of over 97%. We, therefore, conclude that these fluctuations cannot be of tidal origin. In view of the fact that wells 27 and 34 are production wells, we surmise that sudden drops in their water levels are caused by pumping of these or nearby production wells.

HYDROLOGICAL IMPLICATIONS

Tidal lag times and attenuation depend on the tidal period t_o, inland distance x, and the hydraulic transmissivity T and storage coefficient S, in accordance with equations 2 and 3. For unconfined aquifers the storage coefficient S is equal to the effective porosity (Vacher, 1978), which for the karst aquifers of San Salvador is probably close to the actual porosity. Based on previous porosity determinations by Weir and

Kunze (1988) and Kunze and others (1989), a value for S of 0.25 is assumed for this study. Solving equation 3 for hydraulic transmissivity T yields the expression

Equation (14)

$$T=(t_0 S x^2)/(4\pi t_L^2)$$

With the appropriate values for S and t_o corresponding to the semidiurnal tide, T is given by

Equation (15)

$$T=0.247\ (x/t_1)^2$$

The resulting values for T corresponding to semidiurnal lag times t_1 in the seven wells investigated are listed in Table 6. The listed lag times of 8 hours for wells 17, 27 and 34 are minimum lag times consistent with the absence of observed semidiurnal tidal cycles in these wells. Consequently, the resulting corresponding hydraulic transmissivities (T) are maximum values. In view of the fact that the effective porosity (S) may be considerably less than 25%, all calculated values of T, which is directly proportional to S (equation 14), may be too large. Indeed, the calculated hydraulic transmissivities imply hydraulic conductivities K for wells 1, 9, 10, and 18 that are unrealistically high. The hydraulic conductivity K is related to hydraulic conductivity T and saturated aquifer thickness d as

Equation (16)

$$K=T/d$$

Taking a value d of 35 m, which is the approximate average thickness of the main aquifer in the Bahamas, the Lucayan Limestone, on San Salvador (Cant and Weech, 1986), yields the hydraulic conductivity values listed in the last column of Table 6. The values of several m/s for wells 1, 9, 10 and 18 correspond to those for gravel (Freeze and Cherry, 1979) and are much too high for karst limestone. Maximum values of several cm/s implied for wells 17, 27 and 34 are near the upper limit for karst limestone or clean sand (Freeze and Cherry, 1979) and are thus more realistic.

The water level changes recorded in well 27 are thought to reflect draw-down due to pumping of this or an adjacent well during the measurement period (see Figure 4F). Well 27 is a 20 cm diameter unscreened well, 5 m in depth, with about 1.5 m of casing. An independent estimate of hydraulic conductivity (K) and transmissivity (T) can be obtained for this well by considering the fluctuation data as a Hvorslev slug test, where a well is allowed to recover after a volume of water is removed (Freeze and Cherry, 1979). Hydraulic conductivity is calculated from the expression

Equation (17)

$$K = \frac{r^2 \ln(L/R)}{2Lt_r}$$

where r is the casing radius, L and R are the length and radius of the "screen", and t_r is the recovery time. This calculation indicates values of 8×10^{-5} cm/s for hydraulic conductivity and 0.30 cm^2/s for transmissivity. These values are below the expected range for karstic limestone and may indicate that secondary porosity (karst) has not developed in the upper 5 m of this aquifer.

CONCLUSIONS AND FUTURE WORK

Conclusions

The results of this study are ambiguous, unrealistic and inconsistent with theoretical considerations. In at least some cases malfunction of the mechanical tide gauge is indicated (flattened tidal peaks in wells 9 and 10). In addition, later checks of the optical assembly show significant weakening of the rubber diaphragm and changes in the calibration curve which render all recorded water levels unreliable. Nevertheless, the recorded times of well tide extrema appear to be largely unaffected by these problems and may be considered to be reasonably accurate. Thus the resulting improbable hydraulic parameters must have other explanations.

One possibility is that the coastal tides published for San Salvador in the NOAA Tide Tables are not representative of the actual tides along the coast near the well field. This can only be ascertained by actual tide measurements along the coast of San Salvador. Another serious source

of error may be unmodeled sealevel fluctuations caused by meteorological phenomena or by sea water salinity/temperature changes (Vacher, 1978). Again, these nontidal fluctuations can be reliably determined only by actual coastal sealevel measurements. Water levels in wells are also affected by precipitation events and crustal strains, but these effects are probably of minor importance. However, we suspect that the diurnal tidal component cannot be determined reliably because of the unknown magnitude of diurnal groundwater-level changes in response to evapotranspiration.

It may be significant that all estimated semidiurnal tidal lag times are approximately equal and inexplicably small (20-30 min). Similar anomalous tidal phenomena in the Bahamas are reported by Cant (1989): tidal responses in deep wells on Long Island were greater than and occurred in advance of coastal tides, and tidal fluctuations in certain blue holes are out of synchronization with local tides. These well tides are thought to be more closely attuned to those of the deep ocean than to coastal or local tides due to the highly permeable, cavernous nature of the entire island platform which facilitates easier transmission of tidal fluctuations through the deep bedrock of the islands than across the shallow banks.

Future Work

Due to the questionable performance of the mechanical tide gauge used, another sensor system was designed for future use. The new design uses the capacitive effect of an insulated wire strung tight along the center of a 1/2 inch diameter, 60 inch long copper tube. The tube is lowered vertically (partially) into a well. As the water (a conducting medium) rises, the total capacitance of the tube increases, changing the frequency of an alternating current (AC) in the insulated wire. Hence, the recorded AC frequency is a function of water level.

A second, more thorough survey of the study area, utilizing four tide gauges of the new design, is planned for December 1990. In this survey, the coastal tides in Graham's Harbor will be monitored continuously, and coastal tides near the Cockburn Town airstrip will be recorded for at least two tidal cycles in order to better define the tidal forcing function as well as non-tidal sealevel fluctuations during the study period. Water level fluctuations will be recorded for one tidal period or longer in at least ten wells including most or all of the seven wells investigated in this study. In addition, a barometric record of the entire study period will be kept to facilitate separation of tidal water level fluctuations from those of meteorological origin.

ACKNOWLEDGMENTS

The authors wish to thank the Executive Director of the Bahamian Field Station, Dr. Donald T. Gerace for logistical and personal support of this project. We are also grateful to Clifford Fernander for his kind cooperation.

REFERENCES CITED

Cant, R.V., 1989, Geological implications of deep well disposal in the Bahamas: in Mylroie, J.E., ed., Proceedings of the Fourth Symposium on the Geology of the Bahamas: Bahamian Field Station, p. 53-60.

Cant, R.V. and Weech, P.S., 1986, A review of the factors affecting the development of Ghyben-Herzberg lenses in the Bahamas: Journal of Hydrology, v. 84, p. 333-343.

Davis, R.L. and Johnson, Jr., C.R., 1989, Karst hydrology of San Salvador: in Mylroie, J.E., ed., Proceedings of the Fourth Symposium on the Geology of the Bahamas: Bahamian Field Station, p. 118-136.

Ferris, J.G., 1951, Cyclic fluctuations of water level as a basis for determining aquifer transmissibility: Assemblee Generale de Bruxelles, Assoc. Int'l. d'Hydrologie Scientifigue, v. 2, p. 148-155.

Freeze, R.A. and Cherry, J.A., 1979, Groundwater, Prentice-Hall, Englewood Cliffs, NJ, 604 p.

Kunze, A.W.G., Sauter, A.K. and Weir, W.G., 1989, Geoelectrical survey of the Columbus Landings I region of San Salvador, Bahamas: in Mylroie, J.E., ed., Proceedings of the Fourth Symposium on the Geology of the Bahamas: Bahamian Field Station, p. 191-202.

Todd, D.K., 1959, Ground water hydrology: John Wiley and Sons Inc., New York, 336 p.

Vacher, H.L., 1978, Hydrology of small oceanic islands - influence of atmospheric pressure on the water table: Ground Water, v. 16, no. 6, p. 417-423.

Weir, W.G. and Kunze, A.W.G., 1988, Geoelectrical properties of selected rock and water samples from San Salvador Island, Bahamas: Bulletin of the Association of Engineering Geologists, v. 25, p. 255-261.